Resonances

Basic aspects of resonance phenomena and amplitude analysis

A. Augusto Alves Jr

University of Cincinnati
aalvesju@cern.ch

Presented at "YETI 2018: Flavours and Resonances"
IPPP - Durham University, Durham
from 7 to 10 January of 2018

Outline

1. The LHC accelerator and its detectors.
2. Resonances
3. Parametrization of line-shapes
4. Spin formalisms and angular correlations
5. Commented result: $Z(4430)^-$
6. Summary

The LHC and its detectors

The LHC accerates and collides two high luminosity and high energy beams of protons or heavy ions.

- Two general proposal high luminosity experiments: CMS and ATLAS.
- One experiment dedicated to flavour physics: LHCb.
- Heavy-ion experiment: ALICE.

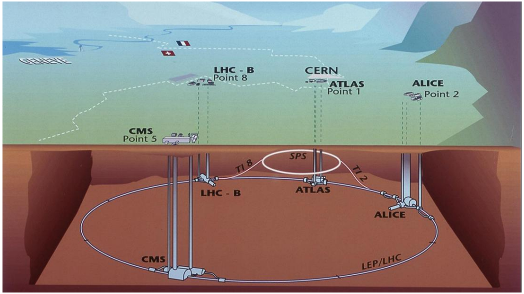

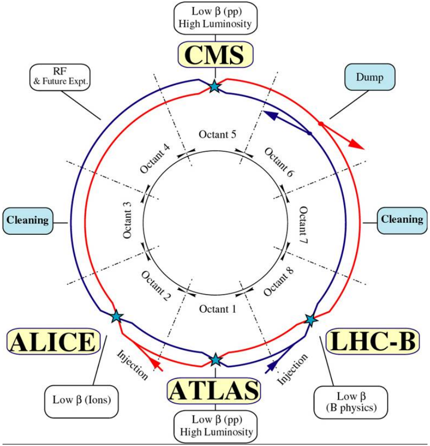

The LHC environment

During most of 2012 run, LHC collided protons at 8 TeV with an average instantaneous luminosity of $4 \times 10^{32} cm^{-2} s^{-1}$ (LHCb) and 20 MHz of bunch crossing.

- Inelastic cross section $\sim 60\,\mathrm{mb}$
- $\sigma(\mathrm{pp} \to \mathrm{b\bar{b}}X) = (284 \pm 20(\mathrm{stat}) \pm 49(\mathrm{syst}))\ \mu\mathrm{b}$
  [PLB 694, 209]
- **$\sim 10^6$ $\mathrm{B\bar{B}}$ produced per second**
- $\sigma(\mathrm{pp} \to c\bar{c}X)$ is about 20 times higher.
  [Nucl.Phys. B871 (2013) 1-20]

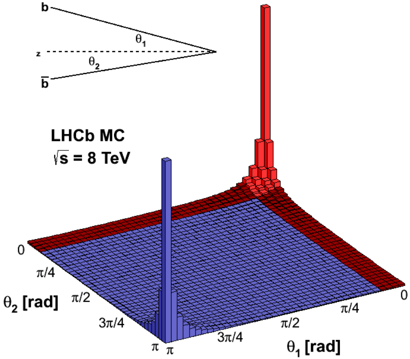

At the LHC energy, the $\mathrm{b\bar{b}}$ pairs are produced preferentially at forward (backward) directions.

- Optimal design is a forward detector: LHCb

The LHCb detector

LHCb experiment is designed to perform high precision flavour physics measurements at the LHC.

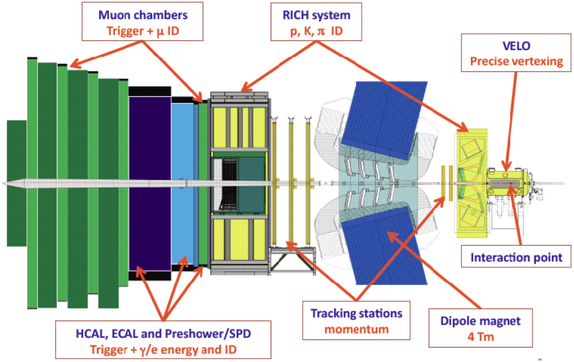

- **Single-arm design.** Covering the range $2 < \eta < 5$, LHCb can exploit the dominant heavy flavour production mechanism at the LHC and detects $\sim 40\%$ of the $b\bar{b}$ produced in forward region.
- **Good particle identification.** Excellent muon identification and good separation of π, K and p over (2 - 100) GeV.
- **Good vertexing and tracking.** Precise primary and secondary vertex reconstruction. Excellent momentum, IP and proper time resolution.
- These same features make LHCb very suitable for precision spectroscopy studies in the forward region.

The operation of the LHCb detector

Runs I and II

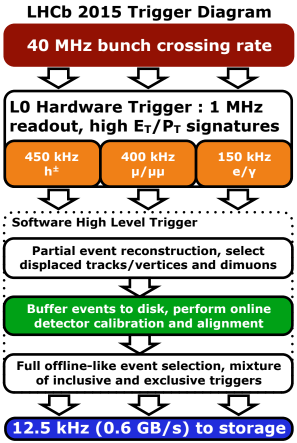

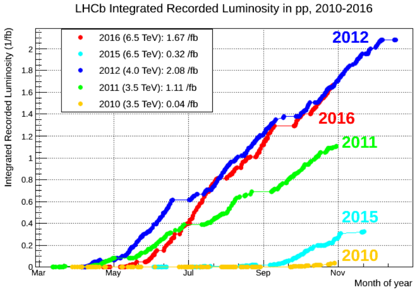

	Run I (2011 + 2012)	Run II (2016)
Bunch spacing	50ns	25ns
E_{cm}	7 TeV/ 8 TeV	13 TeV
Luminosity	$1 + 2\ \text{fb}^{-1}$	$>5\ \text{fb}^{-1}$
Bunches	up to 1262	∼2622

The simplest definition for resonances is that they are extremely short lived particles, with lifetime around 10^{-23} seconds or less. In more technical a way, resonances are poles in the unphysical sheets of the S-matrix, which manifest themselves as structures in experimental observables.

- Usually, resonances show up as peaks in cross-sections and decay density probabilities as a function of the energy.
- The width is also connected to decay channels accessible to the resonance and can also be as small as sub MeV/c^2 or as large as several hundred MeV/c^2.
- Well isolated, relatively narrow and far from the threshold resonances can be described by standard Breit-Wigner parametrization.
- Overlapped or close to the threshold resonances usually require more refined treatment.

The PDG review on resonances and the references therein are good starting points on the subject.

Dimuon invariant mass at LHC

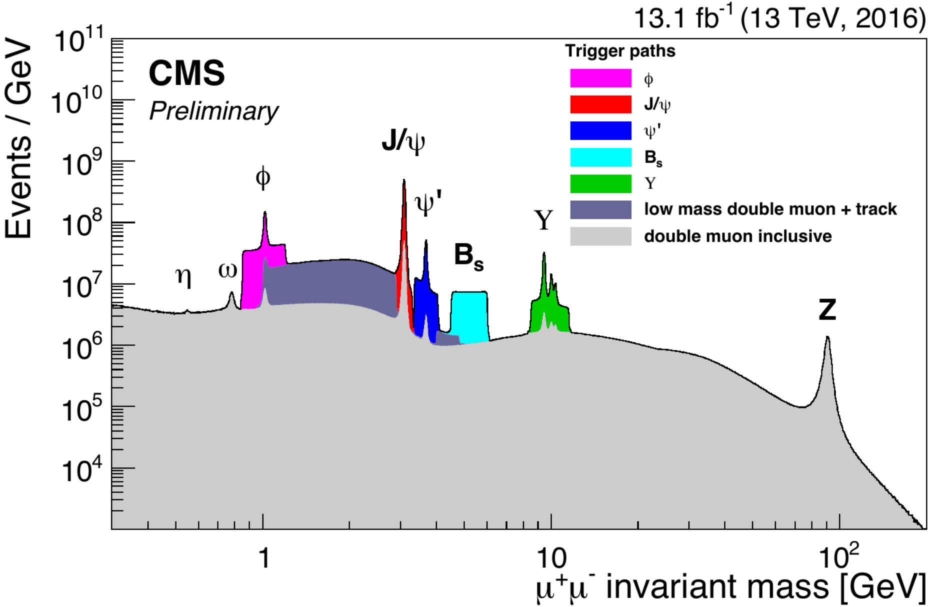

For example, for a single resonance R in $B \to Rc$, with $R \to ab$, one can right

$$\mathcal{A}_{ab} = -\gamma_B(s) \frac{g_B g_R}{s - \widehat{M}_R^2(s) + iM_R(s)\Gamma_R(s)} \gamma_R(s), s = m_{ab}^2$$

- g_B and g_R are phenomenological couplings.
- $\gamma_R(s) = q_R^{L_R} F_{L_R}(q_R, q_{R,0})$. Here L_R denotes the angular momentum of the decay products and F_{L_R} is a phenomenological form factor. The common choice for F_{L_k} are the Blatt-Weisskopf functions.
- $\widehat{M}_R(s) = M_{R,0} + M(s)$ is the mass function. For narrow and isolated resonances: $\widehat{M}_R(s) = M_{R,0}$.
- $\Gamma_R(s)$ is the resonance's width. For narrow and far from threshold resonances: $\Gamma_R(s) = \Gamma_{R,0}$

In summary, for isolated, narrow and far from threshold resonances one can use the standard Breit-Wigner parametrization. The Breit-Wigner parameters M_R and Γ_R agree with the pole parameters only if $M_{R,0}\Gamma_{R,0} \ll \mid M_{thr.}^2 - M_R^2 \mid$.

Multi–particle final states - Isobar model

The basic idea behind the Isobar Model is that any many-body reaction can be modeled as a tree of subsequent two-body decays. So, one can parametrize decays to multi–particle final states in terms of successive decays of two–body resonances.

- The process is dominated by two-body processes.
- Different intermediate states can interfere if the internal tree configuration is not unique given the final state.
- The full amplitude is the coherent sum of all combinations, integrated over all internal degrees of freedom.
- The final probability density for the reaction is integrated over all unobservables.

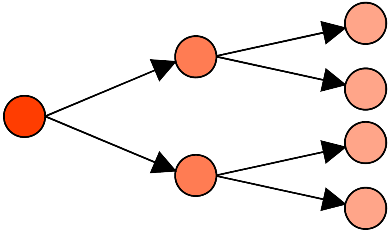

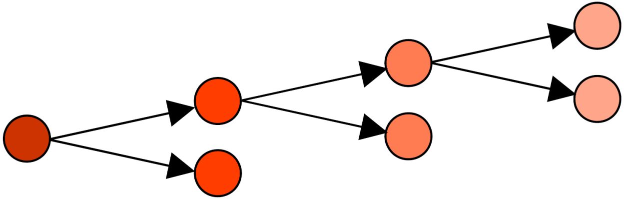

Resonances

Example of observables

Please, consider a decay chain like $B \to Rc$ where R is a resonance decaying to $R \to ab$

Magnitude

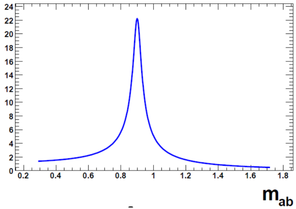

Phase

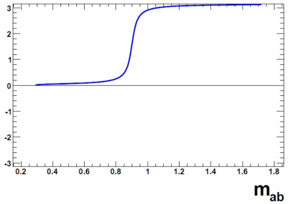

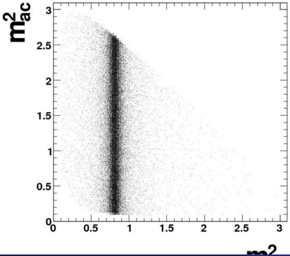

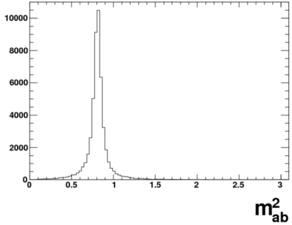

For resonances occurring close to the threshold, one needs to use

$$\Gamma_R(s) = \Gamma_{R,0}\left(\frac{q}{q_0}\right)^{2L_R+1}\left(\frac{M_R}{s}\right)\left(\frac{F_{L_R}(q,q_0)}{F_{L_R}(q_R,q_0)}\right)$$

- Non-constant g_B and g_R couplings and different phenomenological form factors.
- If there are overlapping resonances, it is generally incorrect to use a sum of Breit-Wigner functions. **K-matrix formalism** can be more appropriate.
- Resonances at threshold can be better treated using the **Flatté parametrization**.

If none of these alternatives are enough to get a good description of the data, custom formalisms needs to be developed starting from the general features of the Scattering Theory.

Angular analysis

As with everything else resonances carry quantum numbers and are, of course, also subject to conservation laws. The study of the angular distributions and correlations is mandatory to determine the quantum numbers of the resonances. There are different spin formalisms, but all of them are developed studying the representations of the Poincaré group:

- Non-relativistic tensor formalism (Zemach).
- Spin-projection formalisms.
- Relativistic tensor Formalisms (Rarita-Schwinger).

Zemach formalism

This formalism uses pure spin tensors to avoid the explicit construction of spin wave functions and evaluates the amplitudes always in the rest frame of the decaying particle, avoiding the complications arising from the use of the four-momentum indices.

- It is non-relativistic and gives corrects results only for decays of spinless into spinless final states.
- The angular distributions are proportional to Legendre polynomials on the cosine of the helicity angle, multiplied by powers of pq:

$$Z_L(\theta) \propto (-2qp)^L P_L(cos(\theta))$$

- Fast computation and simple for small orbital angular momentum and spin values
- Very popular among the Dalitz's plot analysts.

Spin-projection formalisms

Basically, one starts with the particle states at rest, then develops the corresponding standard representation of angular momentum and finally applies rotations and "boosts" to obtain states for relativistic particles with arbitrary momentum. In summary, the formalisms developed in this way differ in the choice of the quantization axis.

- **Helicity Formalism**. Quantization axis parallel to the direction of motion. Particle are described at rest by eigenstates of helicity and momentum then ones applies a rotation to direct the quantization axis to the direction of movement followed by a boost in that direction to get the particle with $\vec{p}$

$$|\vec{p}, \lambda\rangle = B(0, 0, p)R(\phi, \theta, -\phi)|\lambda\rangle$$

- **Canonical Formalism**. The quantization axis is diagonal to the direction of motion. The spin z-component is defined only in the particle's rest frame. A boost is applied to obtain the particle with $\vec{p}$:

$$|\vec{p}, s_z\rangle = B(\vec{p})|s_z\rangle$$

- **Tranversality Formalism**. Similar to helicity formalism, but the quantization axis is chosen to be normal to the direction of motion.

Steps to build a spin formalism

Chosen the formalism, from the starting points discussed in the previous slides, one needs:

1. Define the single particle states with given momentum and spin component in the chosen base.
2. Define the two-particle states in the center-of-mass system and the corresponding amplitudes.
3. Define the transformation formulas to states and amplitudes of given total angular momentum.
4. Apply the symmetry restrictions on the amplitude: parity, time-reversal.
5. Derive formulae for observable quantities, distributions etc.

Below an example of three resonances defined by the same line-shape, but with different spins.[1]

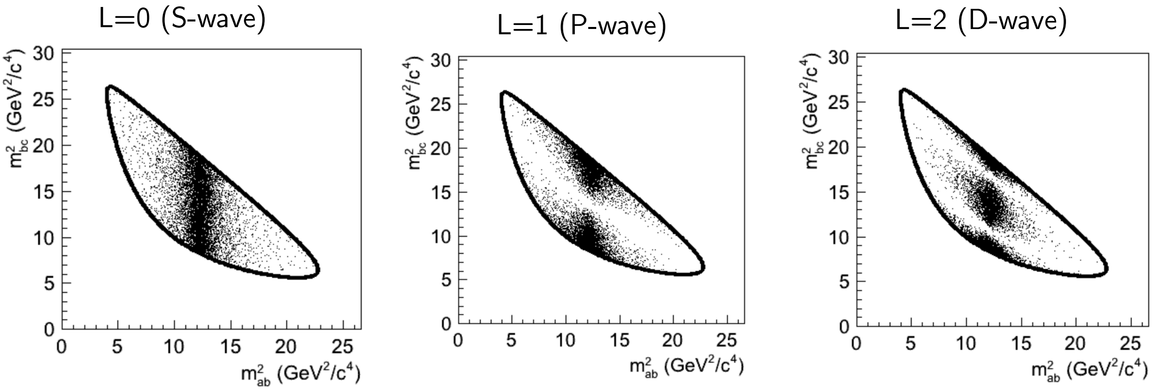

[1] Thanks to A. Poluektov for the figures.

Below an example of three spin-0 resonances defined by the same line-shape, but with different phases between them.[2]

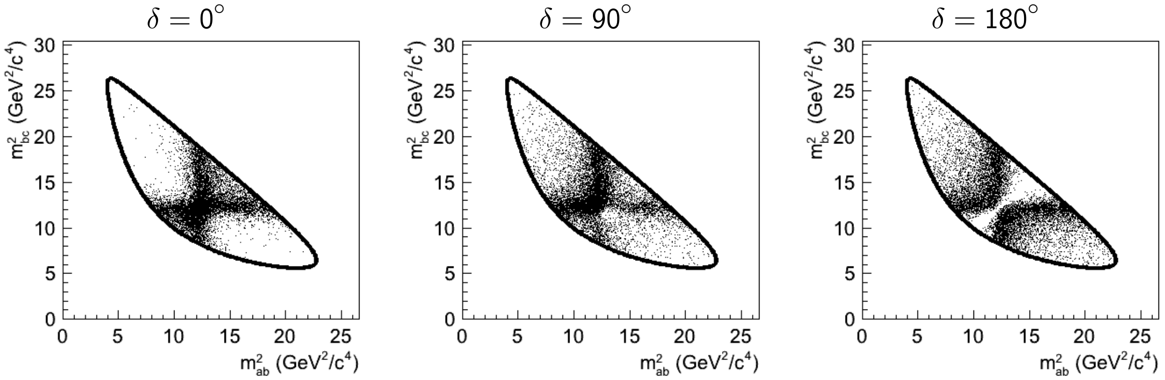

[2] Thanks to A. Poluektov for the figures.

How to measure the quantum numbers of a resonance?

- Be sure the bump you are observing is signal. Efficiency correction, background subtraction, resolution effects...
- Identify the possible quantum number assignments (respect the conservation laws).
- Write down an amplitude and a fit model corresponding to each possible resonance quantum number.
- Go ahead, fit the models and perform hypothesis tests to identify which is the model prefered by data.
- Each model corresponds to a set of quantum numbers for the resonance.

Easier said than done!

- "Charged" charmonium like state decaying into $\psi(2S)\pi^-$ first reported by Belle in $B^0 \to \psi(2S)K^+\pi^-$ decays [Phys.Rev.D88:074026]
- Searched and not confirmed or excluded by BaBar [Phys.Rev.D79:112001]
- Can not be explained as conventional meson.
- Minimum quark content: $c\bar{c}u\bar{d}$
- No corresponding structure observed in $B^0 \to J/\psi K^+\pi^-$

$Z(4430)^-$ at Belle. K^{*0} and $K_2^*(1432)$ vetoed.

With $Z(4430)^-$ and No $Z(4430)^-$

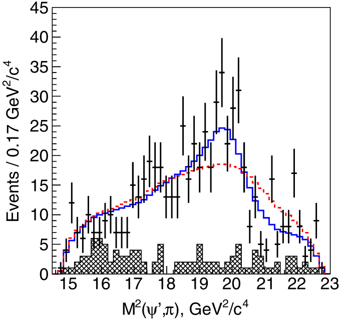

$Z(4430)^-$ at BaBar. Legendre polynomials approach.

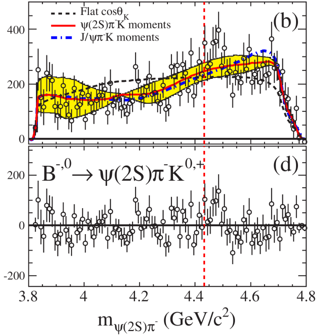

- Sample with >25.000 $B^0 \to K^+\pi^-\psi(2S)$ signal candidates,
- Analysis performed using two different approaches:
  - Model dependent. Four-dimensional amplitude fit (invariant masses, helicity and decay planes angles).
  - Model independent. An analysis based on the Legendre polynomial moments extracted from the $K\pi$ system
- Background from sidebands. Estimated 4% of combinatorial background in the signal region.
- Four-dimensional efficiency calculated using complete simulation of the detector

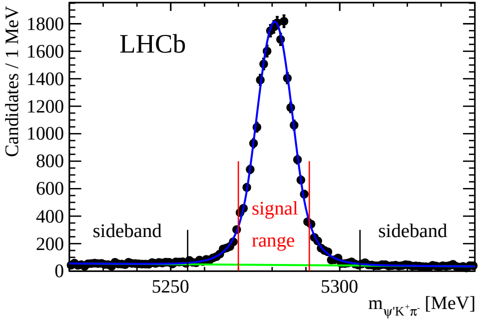

background subtracted Dalitz plot

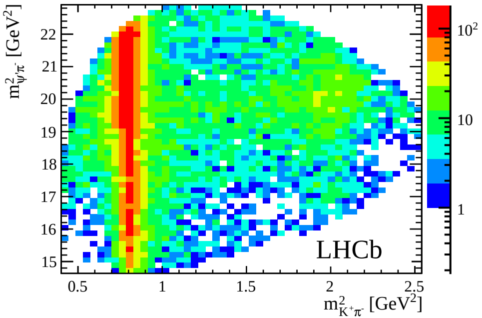

- Two possible decay chains: $\mathrm{B}^0 \to K^{*0}\psi(2S)$ and $\mathrm{B}^0 \to \mathrm{K}^+ Z(4430)^-$ where $K^{*0} \to \mathrm{K}^+\pi^-$, $Z(4430)^- \to \psi(2S)\pi^-$ and $\psi(2S) \to \mu^+\mu^-$
- The decay is described by four independent observables: invariant masses (1), helicity angles (2) and angle between the decay planes (1).
- The angular distributions are calculated using the helicity formalism and resonances are described by Breit-Wigner line-shapes.

$$\left|\mathcal{M}\left(m_{K\pi}, m_{\psi\pi} \middle| \left\{\{\underline{A}_{k,\lambda_\psi}\}_{\lambda_\psi=-1,0,1}, m_{0\,k}, \Gamma_{0\,k}\right\}_{k=K^*\ldots}, \left\{\underline{A}_{Z,\lambda_\psi^Z}\right\}_{\lambda_\psi^Z=-1,0,1}, m_{0\,Z}, \Gamma_{0\,Z}\right)\right|^2$$

$$= \sum_{\Delta\lambda_\mu=-1,1} \left| \sum_{\lambda_\psi=-1,0,1} \sum_k \underline{A}_{k,\lambda_\psi} R(m_{K\pi}|m_{0\,k}, \Gamma_{0\,k}) d^{J_k}_{\lambda_\psi,0}(\theta_{K^*}) e^{i\,\lambda_\psi\,\phi} d^1_{\lambda_\psi,\Delta\lambda_\mu}(\theta_\psi) \right.$$

$$\left. + \sum_{\lambda_\psi^Z=-1,0,1} \underline{A}_{Z,\lambda_\psi^Z} R(m_{\psi\pi}|m_{0\,Z}, \Gamma_{0\,Z}) d^{J_Z}_{0,\lambda_\psi^Z}(\theta_Z) e^{i\,\lambda_\psi^Z\,\phi^Z} d^1_{\lambda_\psi^Z,\Delta\lambda_\mu}(\theta_\psi^Z) e^{i\,\Delta\lambda_\mu\alpha} \right|^2 .$$

The free parameters are the resonance masses, widths and the complex coefficients of the amplitude sum.

$Z(4430)^-$

Amplitude fit

- Fitted parameters:

$$M_{Z(4430)^-} = 4475 \pm 7^{+15}_{-25}\,\mathrm{MeV}/c^2,\ \Gamma_{Z(4430)^-} = 172 \pm 13^{+37}_{-34}\,\mathrm{MeV}/c^2,\ f_{Z(4430)^-} = (5.9 \pm 0.9^{+1.5}_{-3.3})\%$$

.

- Significance: $\Delta(-2lnL) > 13.9\sigma$

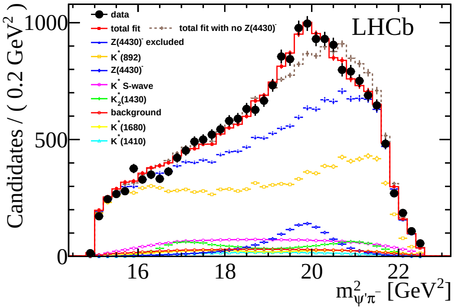

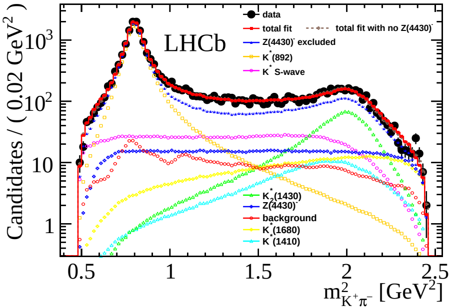

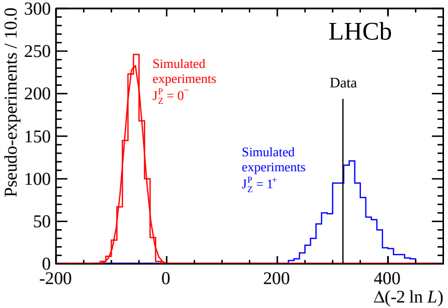

- $J^P = 1^+$ assignment favored.
- Other J^P assignments are ruled out with large significance: $> 9\sigma$

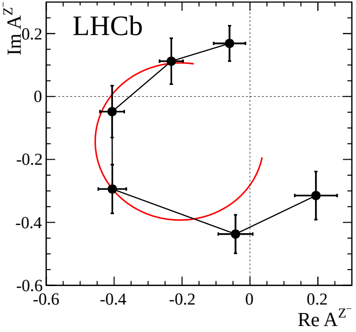

- $Z(4430)^-$ amplitude is described by 6 independent complex numbers instead of a Breit-Wigner
- Observe a fast change of phase crossing maximum of magnitude.
- Expected behaviour for a resonance.

The main goal is to check if the structures in the $m_{\psi(2S)\pi}$ spectrum can be explained as reflections of the resonance activity in the $K\pi$ system.

- No assumptions on the shape and coupling of the K^* resonances.
- Only its maximum J is restricted.

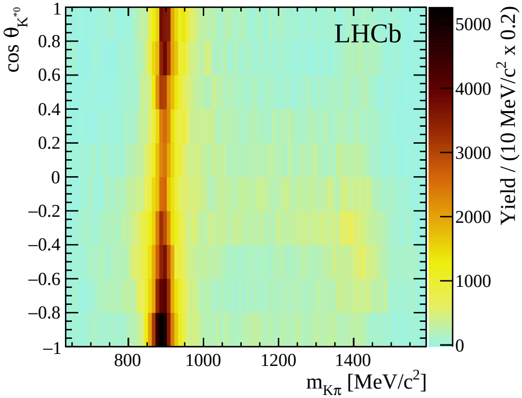

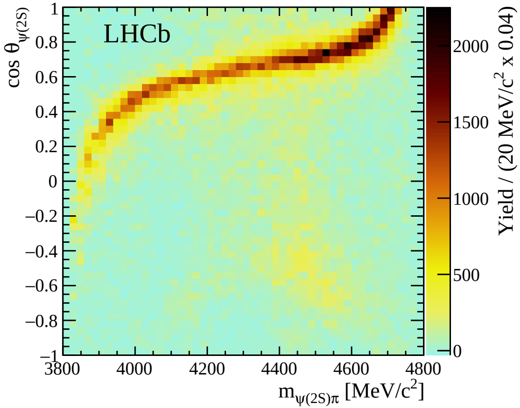

$Z(4430)^-$: model independent analysis

$K\pi$ system

- Very active $K\pi$ system.
- $m_{K\pi}$ taken directly from data, as it is.
- Angular structure of the $K\pi$ system acquired via Legendre polynomials.
- $\frac{dN}{d\cos\theta_{K^{*0}}} = \sum_{j=0}^{l_{max}} \langle P_j^U \rangle P_j(\cos\theta_{K^{*0}})$
- $\langle P_j^U \rangle = \sum_{i=1}^{N_{reco}} \frac{W^i_{signal}}{\epsilon^i} P_j(\cos\theta^i_{K^{*0}})$

Resonance	Mass (MeV/c^2)	Γ (MeV/c^2)	J^P
$K^*(800)^0$	682±29	547±24	0^+
$K^*(892)^0$	895.81±0.19	47.4±0.6	1^-
$K^*(1410)^0$	1414±15	232±21	1^-
$K_0^*(1430)^0$	1425±50	270±80	0^+
$K_2^*(1430)^0$	1432.4±1.3	109±5	2^+
$K^*(1680)^0$	1717±27	322±110	1^-
$K_3^*(1780)^0$	1776±7	159±21	3^-

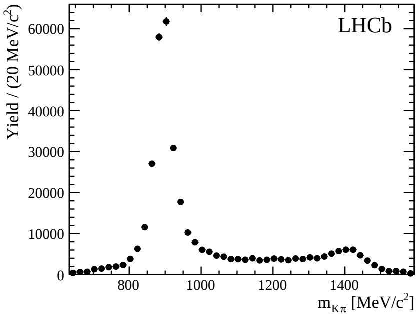

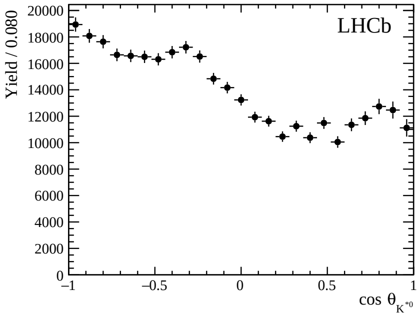

$Z(4430)^-$: model independent analysis

Legendre polynomial moments

The rich angular structure of the $K\pi$ system is shown by the very featured Legendre polynomial moments.

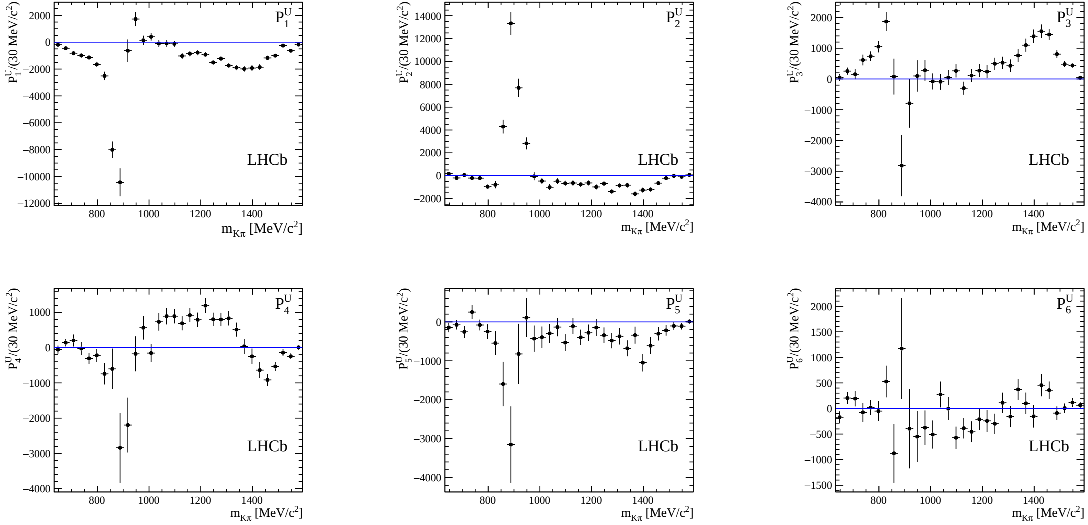

- The moments are normalized and used to predict, through a MC simulation, the expected $\mathrm{m}_{\psi(2S)\pi}$ spectrum.
- The order of the Legendre polynomial expansion depends on the locally dominant $\mathrm{K}\pi$ resonances

$$l_{\mathbf{max}}(\mathrm{m}_{\mathrm{K}\pi}) = \begin{cases} 2 & \mathrm{m}_{\mathrm{K}\pi} < 836\,\mathrm{MeV}/c^2 \\ 3 & 836\,\mathrm{MeV}/c^2 < \mathrm{m}_{\mathrm{K}\pi} < 1000\,\mathrm{MeV}/c^2 \\ 4 & \mathrm{m}_{\mathrm{K}\pi} > 1000\,\mathrm{MeV}/c^2. \end{cases}$$

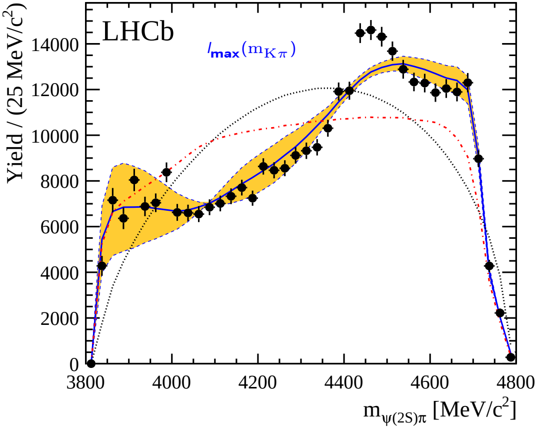

- **Data points(black dots)**
- **MC prediction (blue solid line)**
- Phase space MC (black dotted line)
- Phase space MC weighted to reproduce $\mathrm{m}_{\mathrm{K}\pi}$ (red line)

Slices of $\mathrm{m}_{K\pi}$

Toy Monte Carlo prediction in slices of $\mathrm{m}_{K\pi}$.

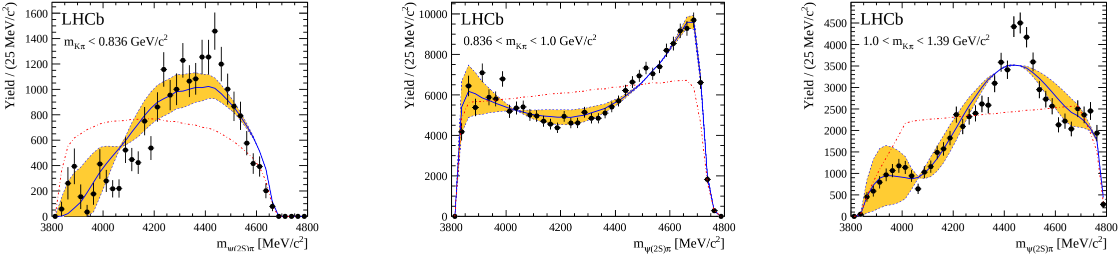

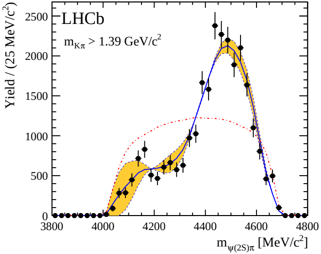

- **Data points(black dots)**
- **MC prediction (blue solid line)**
- Phase space MC weighted to reproduce $\mathrm{m}_{K\pi}$ (red line)
- Clear disagreement between data and MC on the slice $1.0 < \mathrm{m}_{K\pi} < 1.39\,\mathrm{GeV}/c$

$Z(4430)^-$: model independent analysis

Hypothesis test

- Performed using a series of pseudo-experiments produced according with l_{max} $(m_{K\pi})$.
- Hypothesis test based on likelihood ratio between l_{max} $(m_{K\pi})$ and l_{max} $=30$.
- Efficiency effects and background subtraction taken into account in the pseudo-experiment generation.

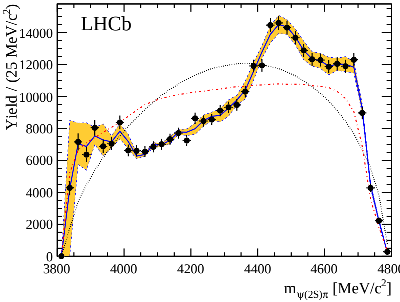

full $m_{K\pi}$ spectrum

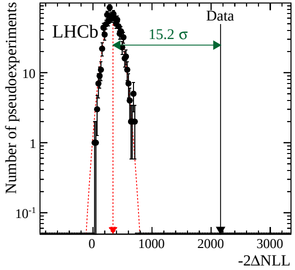

$1.0 < m_{K\pi} < 1.39\,\mathrm{GeV}/c^2$

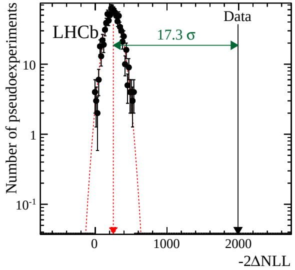

The hypotesis that the structure of the $m_{\psi(2S)\pi}$ spectrum can be described as a reflection of the activity of the resonances in the $K\pi$ system is ruled out with high significance.

Other multidimensional analysis at LHCb

The techniques used in the $Z(4430)^-$ have also been used in a number of other spectroscopy analysis involving the research for new resonances. See Greig's talk after the coffee break:

- Evidence for Exotic Hadron Contributions to $\Lambda_b^0 \to J/\psi\, p\pi^-$ Decays [Phys. Rev. Lett. 117, 082003].
- Observation of $J/\psi\,\phi$ structures consistent with exotic states from amplitude analysis of $B^+ \to \phi K^+$ decays [Phys. Rev. Lett. 118, 022003 (2017)].
- Amplitude analysis of $B^+ \to \phi K^+$ decays [Phys. Rev. D 95, 012002 (2017)].
- Model-independent evidence for $J/\psi\, p$ contributions to $\Lambda_b^0 \to J/\psi\, pK^-$ decays [Phys. Rev. Lett. 117, 082002 (2016)].
- Observation of $J/\psi\, p$ resonances consistent with pentaquark states in $\Lambda_b^0 \to J/\psi\, pK^-$ decays [Phys. Rev. Lett. 115, 072001 (2015)].
- $X(3872)$ quantum numbers determination [Phys. Rev. Lett. 110, 222001 (2013)].
- Evidence of $X(3872) \to \psi(2S)\gamma$ [Nuclear Physics B 886 (2014) 665-680].
- Quantum numbers of the $X(3872)$ state and orbital angular momentum in its $\rho^0 J/\psi$ decays [Phys. Rev. D 92 (2015) 011102].

The concepts connected with resonances are relevant also in other areas: Dalitz plots and CP-violation, New Physics searches etc.

Summary

- Resonance phenomena are very rich. The properties of a resonance are the properties of its complex pole.
- There are many standard parametrizations to describe the line-shape, but unitarity and analyticity should be always kept.
- It is incorrect to use a sum of Breit-Wigner functions: it may violate unitarity constraints.
- Not only about peaks: resonances can create structures in angular distributions and other observables.
- Analysis of angular distributions and correlations is crucial to measure the resonance quantum numbers.

Thank you!